**RAA 2021** Vol. **21** No. **2**, 28(6pp) doi: 10.1088/1674-4527/21/2/28

*http://www.raa-journal.org* *http://iopscience.iop.org/raa*

***R**esearch in*
***A**stronomy and*
***A**strophysics*

# The moment generating function of pairwise velocity in the context of redshift space distortion

Jing-Wei Zhao and Jun-De Chen

Department of Astronomy, Shanghai Jiao Tong University, Shanghai 200240, China; *jundechen@sjtu.edu.cn*

Received 2020 April 23; accepted 2020 May 13

**Abstract** We study the connections between the pairwise velocity moment generating function $G(k_\parallel, \mathbf{r})$ and redshift space distortion (RSD) modeling. Here $k_\parallel$ is the Fourier wavevector parallel to the line of sight, and $\mathbf{r}$ is the pair separation vector. We demonstrate its usage by two examples. (1) Besides the known relations between $G$ and the RSD power spectrum (and the correlation function), we propose a new RSD statistics $P^s(k_\parallel, r_\perp)$ whose connection to $G$ is convenient to evaluate numerically. (2) We then develop a fast method to numerically evaluate $G$, and apply it to a high resolution N-body simulation. We find that $G$ ($\ln G$) shows complicated dependence on $k_\parallel$ beyond the linear and quadratic dependencies. This not only shows inaccuracy in some existing models and identifies sources of inaccuracy but also provides possible ways of improving the RSD modeling. Consequently, more comprehensive investigations on $G$ are needed to fully explore the usage of $G$ in RSD modeling.

**Key words:** cosmology: dark energy — dark matter — large-scale structure of universe

## 1 INTRODUCTION

Redshift space distortion (e.g., Peebles 1980; Kaiser 1987; Scoccimarro 2004) is a powerful cosmological probe. It has made significant contribution in the establishment of the standard ΛCDM cosmology (e.g., Davis & Peebles 1983; Peebles 1984). It continues to be a major scientific target of several major galaxy surveys such as SDSS, 2dF, 6dF, VVDS and BOSS (e.g., Peacock et al. 2001; Tegmark et al. 2004; Guzzo et al. 2008; Reid et al. 2012, 2014). Ongoing/upcoming stage IV surveys such as DESI, PFS, Euclid, SKA (e.g. DESI Collaboration et al. 2016; Amendola et al. 2016; Abdalla et al. 2015) will use redshift space distortion (RSD) to achieve 1% accuracy in measuring the structure growth rate $f(z)\sigma_8(z)$ over multiple redshift bins. Significant further improvement is also possible by more advanced surveys (e.g., Dodelson et al. 2016).

The physics of RSD is straightforward. In a spectroscopic redshift survey, we assign the associated cosmological distance to a given galaxy by assuming the observed redshift as the cosmological redshift. However, since the observed galaxy redshift has an extra Doppler redshift induced by the galaxy peculiar velocity, the measured 3D distribution of galaxies (the so called redshift space distribution), is therefore different from the distribution in real space. This shift in galaxy position happens along the line of sight but not perpendicular to the line of sight. Therefore it renders the otherwise (statistically) isotropic galaxy distribution into anisotropic distribution. By analyzing this characteristic anisotropy, we are able to infer the peculiar velocity of galaxies, without the need of distance indicators and free of the associated systematics. The peculiar velocity field itself is a major measure of the large scale structure (LSS) of the universe, and contains crucial information on dark energy and gravity (e.g., Zhang et al. 2007; Jain & Zhang 2008). This makes RSD one of the major dark energy probes.

A major unresolved problem in RSD cosmology is its theoretical modeling. First, RSD involves both the nonlinear evolution of density field and velocity field, and the nonlinear coupling between the two. Second, the mapping from real space to redshift space is nonlinear. An inevitable consequence is that even the simplest 2-point correlation function in redshift space is determined by not only the 2-point correlation function in real space, but also $n$-point correlation functions ($n > 2$). Over the past three decades, many RSD models (e.g., Peebles 1980; Kaiser 1987; Scoccimarro 2004; Matsubara 2008; Taruya et al. 2010; Seljak & McDonald 2011; Reid & White 2011; Okumura et al. 2012; Zhang et al. 2013; Zheng et al. 2013; Wang et al. 2014; Zheng & Song 2016; Song et al.

2018; Zheng et al. 2019) have been constructed, tested against numerical simulation (e.g., Okumura & Jing 2011; Bianchi et al. 2012; de la Torre & Guzzo 2012; White et al. 2015), and/or applied in the data analysis. Nevertheless, their accuracy at $k \geq 0.1 - 0.2$ h Mpc$^{-1}$ and their applicability to general galaxy samples require more comprehensive studies and independent checks. Furthermore, to fully realize the power of ambitious surveys beyond stage IV (Dodelson et al. 2016), accurate RSD modeling up to $k = 0.4 - 0.5$ h Mpc$^{-1}$ is required. This is beyond the capability of any existing RSD models.

This paper presents an attempt to study RSD, through the viewpoint of pairwise velocity moment generating function. Although we are not able to obtain any solid results directly improving the RSD modeling, the presented results show useful clues/insights for the generating function based RSD modeling, alternative to existing models. This paper is organized as follows. In Section 2, we present the theoretical results linking the pairwise velocity moment generating function to the RSD modeling in configuration space, Fourier space and hybrid space. In Section 3, we use N-body simulation to evaluate the generating function and its dependence on the Fourier wavevector parallel to the line of sight $k_\parallel$. Section 4 discusses the possible implications, summarizes the results, and lists key issues for future works.

## 2 THE PAIRWISE VELOCITY MOMENT GENERATING FUNCTION AND ITS CONNECTION TO RSD MODELING

Redshift space distortion changes the galaxy/DM particle position $\mathbf{x}$ to $\mathbf{s}$,

$$\mathbf{s} = \mathbf{x} + \frac{\mathbf{v}\cdot\hat{x}}{H(z)}\hat{x} = \mathbf{x} + \frac{v_\parallel}{H(z)}\hat{x} \,. \tag{1}$$

Here $H(z)$ is the Hubble parameter at redshift $z$. $v_\parallel$ is the velocity component along the line of sight. For brevity we often neglect this $H(z)$ where it does not cause confusion. The mass/number conservation then leads to an equality

$$(1+\delta(\mathbf{x}))d^3\mathbf{x} = (1+\delta^s(\mathbf{s}))d^3\mathbf{s} \,. \tag{2}$$

In Fourier space we have

$$\begin{aligned}\delta^s(\mathbf{k}) &= \int (1+\delta^s(\mathbf{s}))e^{i\mathbf{k}\cdot\mathbf{s}}d^3\mathbf{s} - (2\pi)^3\delta_{3D}(\mathbf{k}) \\ &= \int \left[(1+\delta(\mathbf{x}))e^{ik_\parallel v_\parallel(\mathbf{x})}\right] e^{i\mathbf{k}\cdot\mathbf{x}}d^3\mathbf{x} - (2\pi)^3\delta_{3D}(\mathbf{k}) \,.\end{aligned} \tag{3}$$

Here $k_\parallel$ is the wavevector component parallel to the line of sight. We have adopted the parallel plane approximation (distant observer approximation) such that the line of sight is a fixed direction. The power spectrum is defined by

$$\langle \delta^s(\mathbf{k})\delta^s(\mathbf{k}')\rangle = (2\pi)^3\delta_{3D}(\mathbf{k}+\mathbf{k}')P^s(\mathbf{k}) \,. \tag{4}$$

We then obtain

$$\begin{aligned}P^s(\mathbf{k}) = &\int \langle (1+\delta_1)(1+\delta_2)e^{ik_\parallel v_{12}}\rangle_{\mathbf{r}'} e^{i\mathbf{k}\cdot\mathbf{r}'}d^3\mathbf{r}' \\ &- (2\pi)^3\delta_{3D}(\mathbf{k}) \,.\end{aligned} \tag{5}$$

Here $\delta_i \equiv \delta(\mathbf{x}_i)$ $(i = 1, 2)$, $\mathbf{r}' \equiv \mathbf{x}_1 - \mathbf{x}_2$, $v_{12} \equiv v_\parallel(\mathbf{x}_1) - v_\parallel(\mathbf{x}_2)$. The ensemble average $\langle\cdots\rangle_{\mathbf{r}'}$ is for fixed pair separation $\mathbf{r}'$. We define a function

$$G(k_\parallel, \mathbf{r}) \equiv \frac{\langle (1+\delta_1)(1+\delta_2)e^{ik_\parallel v_{12}}\rangle}{1+\xi(r)} \,. \tag{6}$$

By definition $|G| \leq 1$. Any non-zero velocity component anywhere in the field will cause $G \neq 1$. The asymmetric component of $v_{12}$ induces an imaginary part. $G$ is the moment generating function of pairwise velocity (Scoccimarro 2004), since

$$\langle v_{12}^m\rangle \equiv \frac{\langle (1+\delta_1)(1+\delta_2)v_{12}^m\rangle}{1+\xi(r)} = \left.\frac{\partial^m G}{\partial(ik_\parallel)^m}\right|_{k_\parallel=0} \,, \; m \geq 1 \,. \tag{7}$$

This moment generating function $G$ determines the redshift space power spectrum

$$P^s(\mathbf{k}) = \int \left[(1+\xi(r'))G(k_\parallel, \mathbf{r}') - 1\right] e^{i\mathbf{k}\cdot\mathbf{r}'}d^3\mathbf{r}' \,. \tag{8}$$

Here for the purpose of numerical evaluation, we have moved the $(2\pi)^3\delta_{3D}(\mathbf{k})$ in Equation (5) into the integral. Furthermore, $G$ is related to the pairwise velocity probability distribution function (PDF), and the RSD modeling in configuration space (correlation function). By multiplying both sides of Equation (8) with $\int \exp(-i\mathbf{k}\cdot\mathbf{r})d^3\mathbf{k}/(2\pi)^3$ and performing the integral, we obtain the redshift space correlation function

$$\begin{aligned}&1+\xi^s(\mathbf{r} = (r_\parallel, \mathbf{r}_\perp)) \\ &= \int (1+\xi(\mathbf{r}' = (r'_\parallel, \mathbf{r}_\perp))p(v_{12}|\mathbf{r}' = (r'_\parallel, \mathbf{r}_\perp))dr'_\parallel \,, \\ &\quad v_{12} = r_\parallel - r_\parallel' \,.\end{aligned} \tag{9}$$

Here $p(v_{12}|\mathbf{r})$ is the pairwise velocity PDF. This is related to $G$ by

$$p(v_{12}|\mathbf{r}) = \int G(k_\parallel, \mathbf{r})e^{ik_\parallel v_{12}}\frac{dk_\parallel}{2\pi} \,. \tag{10}$$

Although these results have been known in the literature (e.g., Scoccimarro 2004), to our knowledge no one directly evaluated $G$ and compared it with numerical simulations in the context of RSD. Consequently, this will be a major focus of this paper. Equation (9) is the streaming model widely adopted in RSD modeling. If we adopt a Gaussian $p(v_{12})$ with nonzero $\langle v_{12}\rangle$, then we obtain the Gaussian streaming model (Reid & White 2011).

Interestingly, if we multiply both side of Equation (8) with $\int \exp(-i\mathbf{k}_\perp \cdot \mathbf{r}_\perp) d^2\mathbf{k}_\perp/(2\pi)^2$ instead, we obtain

$$P^s(k_\parallel, r_\perp) = \int \left[(1+\xi(r))G(k_\parallel, \mathbf{r}) - 1\right] e^{ik_\parallel r_\parallel} dr_\parallel \ . \tag{11}$$

This is neither the correlation function nor the power spectrum. But this hybrid statistics has some attractive features. (1) $P^s(k_\parallel = 0, r_\perp) = P(k_\parallel = 0, r_\perp) = w_p(r_\perp)$. Namely the $k_\parallel = 0$ mode is unaffected by RSD, and its value equals to projected correlation function. So RSD is constrained to $k_\parallel \neq 0$ modes. This is an advantage that $\xi^s$ does not share. (2) The modeling of $G(k_\parallel, \mathbf{r})$ is expected to be more straightforward than $p(v_{12}|\mathbf{r})$. So the modeling of $P^s(k_\parallel, r_\perp)$ can be easier than $\xi^s(r_\parallel, r_\perp)$. Meanwhile, the measurement of $P^s(k_\parallel, r_\perp)$ is as straightforward as $\xi^s(r_\parallel, r_\perp)$. Therefore working with $P^s(k_\parallel, r_\perp)$ directly is a promising alternative to $P^s(k_\parallel, k_\perp)$ and $\xi^s(r_\parallel, r_\perp)$.

Equations (8), (9) and (11) then motivate us to numerically investigate the moment generating function $G$. We expect that this may provide new insight on the RSD modeling. Furthermore, starting with the pairwise velocity generating function instead of $p(v_{12}|\mathbf{r})$ has certain advantages. First, the parameterization of $p(v_{12}|\mathbf{r})$ is not straightforward and cannot be easily obtained by Taylor expansion or other familiar tools. However, $G$ and $\ln G$ can be conveniently expanded into its Taylor series in which coefficients are the pairwise velocity moments/cumulants. Second, it is less studied compared to $p(v_{12}|\mathbf{r})$ and therefore there may be still useful information to be revealed. Third, in RSD, we often decompose the peculiar velocity into a large scale component $v_L$ (bulk flow) and a small scale component $v_S$ (random motion) because the two have different impacts on RSD. We can write $v_{12} = v_{12,L} + v_{12,S}$ where $v_{12,L}$ and $v_{12,S}$ are independent to each other. Then the PDF of $v_{12}$ is the convolution of the PDFs of $v_{12,L}$ and $v_{12,S}$,

$$p(v_{12}|\mathbf{r}) = \int p(v_{12,L}|\mathbf{r}) p(v_{12,S}|\mathbf{r}) \delta_D(v_{12,L} + v_{12,S} - v_{12}) dv_{12,L} dv_{12,S} \ . \tag{12}$$

In combination with Equation (10) and its inverse Fourier transformation, we are then able to prove a potentially useful relation

$$G(k_\parallel, \mathbf{r}) = G_L(k_\parallel, \mathbf{r}) G_S(k_\parallel, \mathbf{r}) \ . \tag{13}$$

Here $G_{L,S}$ are the generating functions of $v_{12,L}$ and $v_{12,S}$ respectively. We show one example why this relation is useful. By plugging it into Equation (11), we obtain

$$P^s(k_\parallel, r_\perp) \simeq \left\{ \int \left[(1+\xi(r))G_L(k_\parallel, \mathbf{r})\right] e^{ik_\parallel r_\parallel} dr_\parallel \right\} \times G_S(k_\parallel, \mathbf{r} = (0, r_\perp)) \ . \tag{14}$$

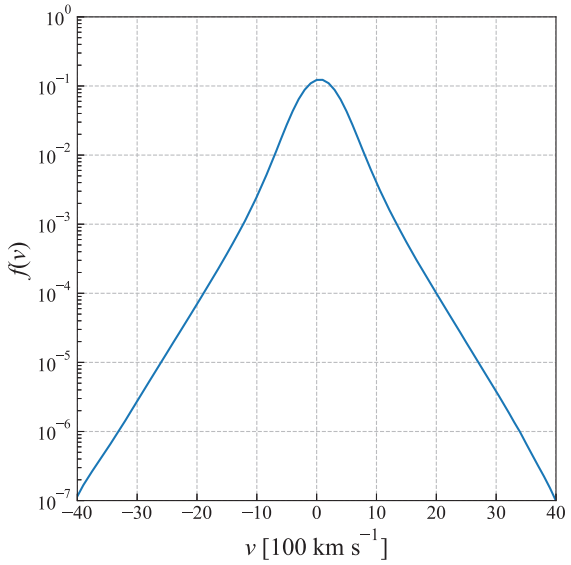


**Fig. 1** The probability distribution function of the one-dimensional velocity ($v_{x,y,z}$), evaluated with a $3072^3$ simulation of ΛCDM cosmology at $z = 0$. The PDF is clearly non-Gaussian, with a long tail of $|v| \gg \sigma_v$ and of the asymptotic exponential PDF $\propto \exp(-|v|/v_*)$.

We can move $G_S$ out of the Fourier transform, for two reasons. First, this is a small scale velocity mode, whose spatial correlation is weak and only exists below certain $r$. Second, due to $r_\perp \neq 0$, only spatial correlation at $r \geq r_\perp$ contributes to $P^s(k_\parallel, r_\perp)$. Consequently, by appropriate choice of $r_\perp$, we can set $G_S(k_\parallel, \mathbf{r}) = G_S(k_\parallel, \mathbf{r} = (0, r_\perp))$ and obtain the above result.

## 3 NUMERICAL EVALUATION OF THE PAIRWISE VELOCITY MOMENT GENERATING FUNCTION

We analyze one of the CosmicGrowth simulation series (Jing 2019), which was denoted J6620 in our previous works (e.g., Chen et al. 2018). The simulation runs with a P$^3$M code (Jing et al. 2007), boxsize $L_{\rm box} = 1200\ {\rm h}^{-1}$ Mpc, and $N_P = 3072^3$ simulation particles. It adopts the standard ΛCDM cosmology, with $\Omega_m = 0.268$, $\Omega_\Lambda = 0.732$, $\Omega_b = 0.044$, $\sigma_8 = 0.83$, $n_s = 0.96$ and $h = 0.71$. Figure 1 shows the one point PDF of peculiar velocity $v_\parallel$ (namely $v_{x,y,z}$ in the simulation coordinate system). The one point PDF clearly shows that the velocity distribution is non-Gaussian, with a power-law like long tail of high velocity $v \gtrsim 3000$ km s$^{-1}$. Furthermore, as shown in the literature (e.g., Scoccimarro 2004), the pairwise PDF is asymmetric, reflecting the mean pairwise velocity $\langle v_{12} \rangle \neq 0$.

For $N_k$ values of $k_\parallel$ of interest, the brute force measurement of $G$ takes $\mathcal{O}(N_P^2 N_k)$ steps. This is too time-consuming. So we design a fast evaluation method

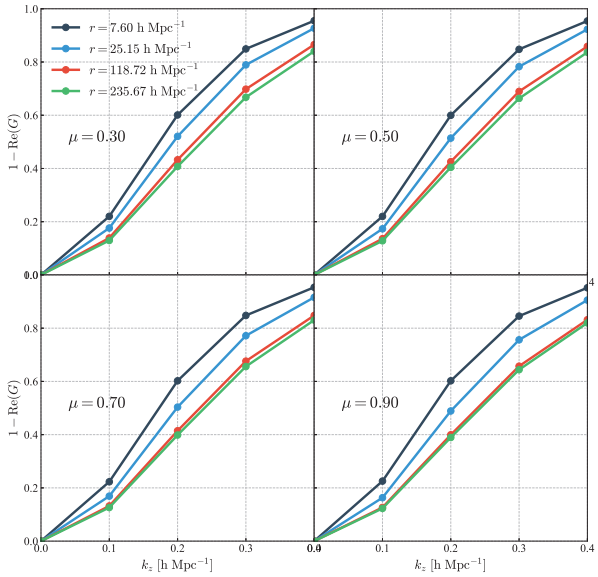


**Fig. 2** Real part of generating function as the function of $k_z$ ($k_\parallel = k_{x,y,z}$). We select four different $r$ values corresponds to lines with different colors. The dependence on $k_z$ is complicated, meaning that simply leading order Taylor expansion in $G$ is not an excellent approximation.

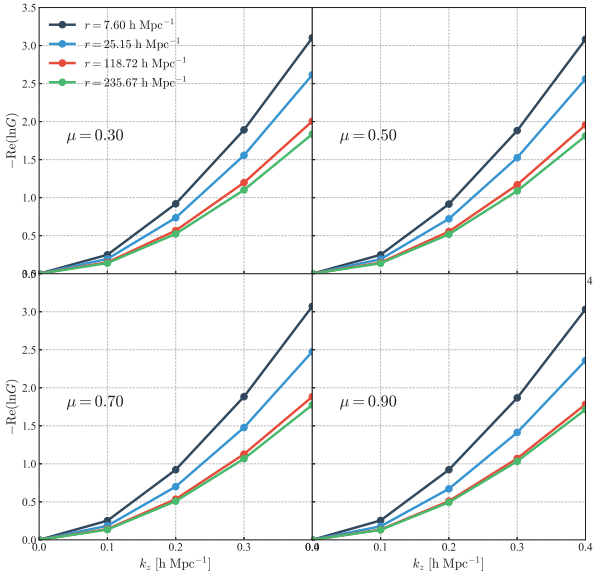


**Fig. 3** Real part of generating function as the function of $k_z$. Comparing to $1-\mathrm{Re}(G)$, $\mathrm{Re}(\ln G)$ is better approximated by $\propto k_\parallel^2$. Nevertheless, the $k_\parallel^2$ behavior is only approximate.

with the aid of FFT. **Step 1**. First we assign particles by the nearest grid point (NGP) method to uniform grid of $N_c = 1024^3$ cells (cell size $L_c = 1.17$ h Mpc$^{-1}$). Each cell then has an estimated overdensity $\hat{\delta} = \sum_i / \bar{n} - 1$, where the sum is over all particles within this cell. $\bar{n} = 3^3$ is the mean number of simulation particles per cell. For a given $k_\parallel$, we also have a field $\hat{p} = \sum_j \exp(ik_\parallel v_{\parallel,j})/\bar{n}$, summing over the same particles. In the continuum limit, this approaches $(1+\delta)\exp(ik_\parallel v_\parallel)$. We choose the line of sight direction as either one of the $x, y, z$ simulation axes. **Step 2**. We evaluate $\langle\hat{\delta}_1\hat{\delta}_2\rangle$ and $\langle\hat{p}_1\hat{p}_2^*\rangle$ by FFTs. The first FFT is $\hat{\delta}(\mathbf{x}) \to \hat{\delta}(\mathbf{k})$. The second is an inverse FFT, $\hat{\delta}(\mathbf{k})\hat{\delta}^*(\mathbf{k}) \to \langle\hat{\delta}_1\hat{\delta}_2\rangle_\mathbf{r}$. We perform the same for $\hat{p}$ and obtain $\langle\hat{p}_1\hat{p}_2\rangle_\mathbf{r}$. We then obtain

$$\hat{G}(k_\parallel, \mathbf{r}) = \left.\frac{\langle\hat{p}_1\hat{p}_2^*\rangle_\mathbf{r}}{1+\langle\hat{\delta}_1\hat{\delta}_2\rangle_\mathbf{r}}\right|_{\mathrm{FFT}} . \quad (15)$$

For each $k_\parallel$, it takes four FFTs to obtain $G(k_\parallel, \mathbf{r})$ at $N_c$ configurations of $\mathbf{r}$. The total computation reduces to a $\mathcal{O}(N_c \log_2(N_c) N_k)$ process. **Step 3**. We then repeat for other values of $k_\parallel$. To avoid spatial smoothing effect caused by the grid assignment, the scale investigated must satisfy $r \gg L_c$. Therefore in this paper we only focus on $r \gtrsim 7$ h Mpc$^{-1}$.

### 3.1 The Real Part of $G$ and $\ln G$

Since $|G| \leq 1$, we plot $1-\mathrm{Re}(G)$ (the real part of $1-G$) in Figure 2. The result shown is at $z = 0$, as a function of $k_\parallel \leq 0.4$ h Mpc$^{-1}$. $G$ also depends on both the amplitude of $\mathbf{r}$ and $u_r \equiv r_\parallel/r$. So we show four values of $r = 7.6$, 25, 119 and 236 h$^{-1}$ Mpc, and four values of $u_r = 0.3, 0.5, 0.7, 0.9$. Figure 2 shows that $1-\mathrm{Re}(G)$ has a complicated dependence on $k_\parallel$, $r$ and $u_r$. According to Equations (6) and (7), $1-\mathrm{Re}(G)$ only contains terms $k_\parallel^{2n}$ ($n \geq 1$) and the leading order term is $k_\parallel^2$. Figure 2 shows that the $k_\parallel^2$ dependence is not a good approximation at all. The slowdown of $1-\mathrm{Re}(G)$ at large $k_\parallel$ means that $k_\parallel^4$ term (with a sign opposite to the $k_\parallel^2$ term) will become important. $1-\mathrm{Re}(G)$ in general decreases with increasing $r$, for fixed $k_\parallel$ and $u_r$. This approaches the limit of no spatial correlation in $v_{1,2}$ when $r \gtrsim 100$ Mpc. The dependence on $u_r$ is weak, although visible. This dependence is caused by the anisotropy in the pairwise velocity moments, whose leading order dependence on $u_r^2$ is $1 + u_r^2(\psi_\parallel/\psi_\perp - 1)$. Since $\psi_\parallel$ and $\psi_\perp$ (the one-dimensional velocity correlation for the cases of $r_\perp = 0$ and $r_\parallel = 0$ respectively) do not differ significantly, the dependence on $u_r$ is weak in $G$. Figure 3 shows the dependence of $\mathrm{Re}(\ln G)$ on $k_\parallel$. The dependence now looks more regular, and $\mathrm{Re}(\ln G) \propto k_\parallel^2$ is a better approximation than that in $1-\mathrm{Re}(G)$. Nevertheless, closer investigations show deviation beyond the $k_\parallel^2$ behavior.

### 3.2 The Imaginary Part of $G$ and $\ln G$

Figures 4 and 5 show the imaginary part of $G$ and $\ln G$. The $k_\parallel$ dependence is even more complicated. This differs from $\propto k_\parallel$ (the first order Taylor expansion) significantly.

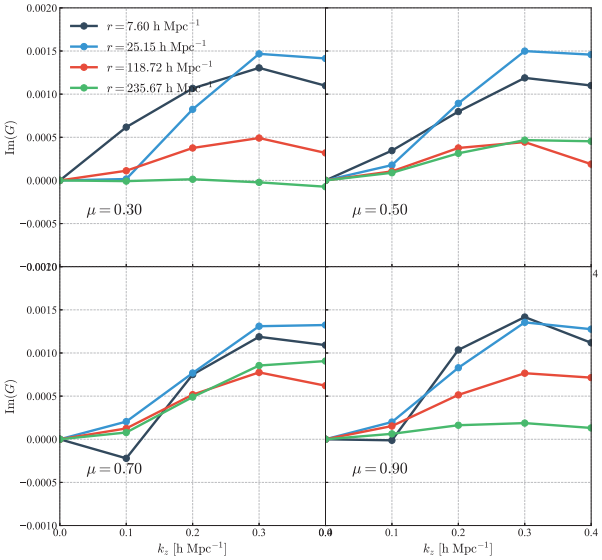


**Fig. 4** Same to Fig. 2, but for the imaginary part.

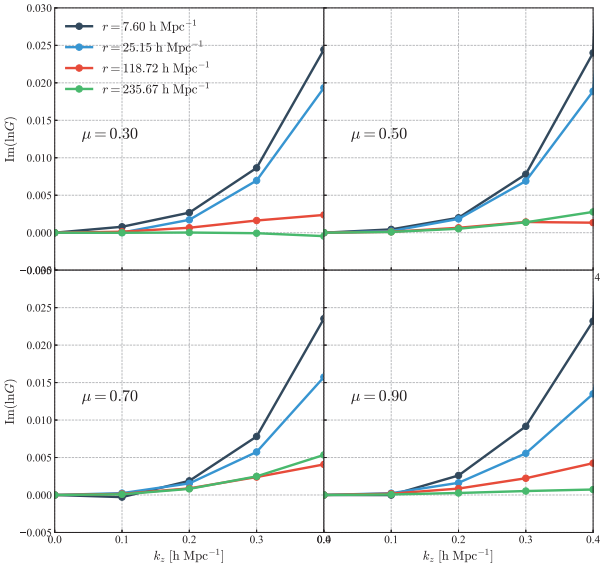


**Fig. 5** Same to Fig. 3, but for the imaginary part. The deviation of Im$(\ln G)$ from the $k_\parallel$ dependence leads to inaccuracy of the Gaussian streaming model. But it also suggests possible ways to improve.

The imaginary part of $G$ is caused by mean pairwise velocity and other higher order odd pairwise velocity moments. The complexity shown here demonstrates a better understanding and modeling of these terms. The Gaussian streaming model assumes a Gaussian $p(v_{12})$, which is equivalent to $\ln G = ik_\parallel\langle v_{12}\rangle - k_\parallel^2\sigma_{12}^2/2$. Here $\sigma_{12}^2 \equiv \langle v_{12}^2\rangle - \langle v_{12}\rangle^2$. The deviation of Re$(\ln G)$ from the $k_\parallel^2$ dependence and the deviation of Im$(\ln G)$ from the $k_\parallel$ dependence clearly suggest the limitation of Gaussian streaming model but it also suggests possible ways to improve. This example demonstrates the usage of pairwise generating function in RSD modeling.

## 4 DISCUSSIONS AND CONCLUSIONS

We highlight the connection between the pairwise velocity generating function $G(k_\parallel, \mathbf{r})$ and the power spectrum $P^s(k_\parallel, k_\perp)$ (and the correlation function $(\xi^s(r_\parallel, r_\perp))$) in redshift space. We also propose a hybrid statistics $P^s(k_\parallel, r_\perp)$, and connect it with $G$. By directly evaluating and understanding $G$ in the context of RSD, we hope to improve the RSD modeling. As a first attempt, we developed a quick evaluation method of $G$, and applied it to a high resolution ($3072^3$ simulation particle) simulation. The measured $G$ shows rich features in the $k_\parallel$ and $\mathbf{r}$ space. Since $G$ directly determines the RSD statistics, these features must be well understood for accurate RSD modeling. For example, Im$(\ln G)$ shows significant departure from the linear $k_\parallel$ dependence, suggesting inaccuracy in the Gaussian streaming model widely used in RSD data analysis. This is certainly an issue for future investigation.

There are many important issues to be investigated in future works. (1) We need to appropriately estimate the cosmic variance in $G$. We plan to use the three CosmicGrowth simulations of $3072^3$ particles and $L_{\rm box} = 600$ h$^{-1}$Mpc (Jing 2019) for this purpose. Together with three independent directions, we will have nine independent samples to evaluate $G$ and its cosmic variance. (2) We will evaluate the redshift dependence of $G$ and pay more attention to $z \sim 0.5 - 1.5$ of great interest for future spectroscopic redshift surveys such as DESI, PFS, Euclid and SKA. (3) More importantly, we will focus more on the halo/subhalo pairwise velocity moment generating function. These are more closely related to the observed galaxy RSD. The difference between the halo pairwise velocity $G$ and the dark matter $G$ can be highly non-trivial, due to the halo definition and the associated inhomogeneous smoothing of the velocity field. (4) We need to quantify the contribution from individual moments (cumulants) to $G$ ($\ln G$). We also need to propagate errors in $G$ to errors in $P^s(k_\parallel, k_\perp)$ and $P^s(k_\parallel, r_\perp)$, so are those in $p(v_{12}|\mathbf{r})$ and $\xi^s(r_\parallel, r_\perp)$.

**Acknowledgements** This work was supported by the National Natural Science Foundation of China (Grant No. 11621303).

## References

Abdalla, F. B., Bull, P., Camera, S., et al. 2015, Proceedings of Advancing Astrophysics with the Square Kilometre Array (AASKA14), 17

Amendola, L., Appleby, S., Avgoustidis, A., et al. 2016, arXiv:1606.00180

Bianchi, D., Guzzo, L., Branchini, E., et al. 2012, arXiv:1203.1545
Chen, J., Zhang, P., Zheng, Y., et al. 2018, ApJ, 861, 58
Davis, M., & Peebles, P. J. E. 1983, ApJ, 267, 465
de la Torre, S., & Guzzo, L. 2012, arXiv:1202.5559
DESI Collaboration, Aghamousa, A., Aguilar, J., et al. 2016, arXiv:1611.00036
Dodelson, S., Heitmann, K., Hirata, C., et al. 2016, arXiv:1604.07626
Guzzo, L., Pierleoni, M., Meneux, B., et al. 2008, Nature, 451, 541
Jain, B., & Zhang, P. 2008, Phys. Rev. D, 78, 063503
Jing, Y. 2019, Science China Physics, Mechanics, and Astronomy, 62, 19511
Jing, Y. P., Suto, Y., & Mo, H. J. 2007, ApJ, 657, 664
Kaiser, N. 1987, MNRAS, 227, 1
Matsubara, T. 2008, Phys. Rev. D, 77, 063530
Okumura, T., & Jing, Y. P. 2011, ApJ, 726, 5
Okumura, T., Seljak, U., McDonald, P., & Desjacques, V. 2012, J. Cosmol. Astropart. Phys., 2, 10
Peacock, J. A., Cole, S., Norberg, P., et al. 2001, Nature, 410, 169
Peebles, P. J. E. 1980, The Large-scale Structure of the Universe, ed. Peebles, P. J. E.
Peebles, P. J. E. 1984, ApJ, 284, 439
Reid, B. A., Seo, H.-J., Leauthaud, A., et al. 2014, MNRAS, 444, 476
Reid, B. A., & White, M. 2011, MNRAS, 417, 1913
Reid, B. A., Samushia, L., White, M., et al. 2012, arXiv:1203.6641
Scoccimarro, R. 2004, Phys. Rev. D, 70, 083007
Seljak, U., & McDonald, P. 2011, J. Cosmol. Astropart. Phys., 2011, 039
Song, Y.-S., Zheng, Y., Taruya, A., & Oh, M. 2018, J. Cosmol. Astropart. Phys., 2018, 018
Taruya, A., Nishimichi, T., & Saito, S. 2010, Phys. Rev. D, 82, 063522
Tegmark, M., Blanton, M. R., Strauss, M. A., et al. 2004, ApJ, 606, 702
Wang, L., Reid, B., & White, M. 2014, MNRAS, 437, 588
White, M., Reid, B., Chuang, C.-H., et al. 2015, MNRAS, 447, 234
Zhang, P., Liguori, M., Bean, R., & Dodelson, S. 2007, Physical Review Letters, 99, 141302
Zhang, P., Pan, J., & Zheng, Y. 2013, Phys. Rev. D, 87, 063526
Zheng, Y., & Song, Y.-S. 2016, J. Cosmol. Astropart. Phys., 2016, 050
Zheng, Y., Song, Y.-S., & Oh, M. 2019, J. Cosmol. Astropart. Phys., 2019, 013
Zheng, Y., Zhang, P., Jing, Y., Lin, W., & Pan, J. 2013, Phys. Rev. D, 88, 103510